Journal of Sound and Vibration (1979) 63(1), 125–143

MATHEMATICAL MODELING OF MULTICYLINDER COMPRESSOR DISCHARGE SYSTEM INTERACTIONS

R. SINGH† AND W. SOEDEL

Ray W. Herrick Laboratories, Purdue University, West Lafayette, Indiana 47907, *U.S.A.*

(*Received* 27 *May* 1978, *and in revised form* 28 *September* 1978)

Gas oscillations are complicated in a multicylinder compressor discharge system because of the cylinder interactions. These are identified and modeled here as kinematic and geometric types of coupling. The kinematic coupling effect is incorporated with the input volume velocities, at the values, which are derived from the discharge mass flow rates. To account for the geometric interactions arising because of the interconnected cavities and passages, impedance matrices are formulated. The discharge system components are described by steady state acoustic impedances, in distributed parameters format. The overall discharge system mathematical model (in the frequency domain) is then coupled with the time domain compressor cylinder thermodynamic, and valve fluid and structural dynamic models. An iterative procedure is used to account for the back pressure effect.

The theory is applied to a two cylinder high speed refrigeration compressor. Unsteady flow pressures are predicted in the valve chamber (for capacity and energy consumption considerations), and at the manifold end (for muffling effectiveness consideration). Excellent agreements between theory and experiment are obtained. The technique as outlined in this paper should be applicable to any multicylinder/interstaged positive displacement type of fluid machine.

1. INTRODUCTION

1.1. GENERAL

Recent investigations [1–6] have demonstrated the interactive nature of the basic processes of a positive displacement compressor. Fluid pressure pulsations play an important role in influencing it. For example, consider a single cylinder with suction and discharge pipes. Unsteady flows in suction/discharge pipes are generated by the reciprocating action of the piston, aided by the rapid opening and closing of pressure actuated automatic valves. These pressure fluctuations, in turn, affect valve displacements, cylinder pressure and instantaneous fluid flow rates. Because of these dynamic interactions, a simultaneous solution of mathematical models describing all basic processes has gained acceptance as a recommended procedure [7, 8]. In multicylinder compressors, these dynamic interactions are further complicated because of the cylinder interactions. Suction/discharge piping of a cylinder influences unsteady flows in the suction/discharge pipings of other cylinders.

1.2. LITERATURE REVIEW

Gas pulsations models usually consist of equations of motion describing unsteady fluid behavior, and are solved to satisfy piping configurations and boundary conditions. Various modeling philosophies have been used with varied degrees of accuracy and completeness

† Now at Carlyle Compressor Company, Carrier Corporation, P.O. Box 4803, Syracuse, New York 13221, U.S.A.

0022-460X/79/050125 + 19 $02.00/0

for pulsation prediction. Linear acoustic theories [1, 3, 5, 6] and the gas dynamic method of characteristics [2, 4] are the two most widely accepted modeling concepts. Practically all of the pulsation models are based on a one dimensional description of the unsteady flow motion. This assumption is valid as only the lower frequencies are of importance and, furthermore, one often encounters small components in high speed reciprocating compressors.

A complete literature review of analysis and simulation of the gas oscillations can be found in references [7] and [8].

The work in the area of modeling of multicylinder fluid machinery manifolds is very limited. Soedel *et al.* [5] applied an acoustic lumped parameters approach to simulate two cylinder refrigeration compressor discharge system interactions. It is described in the time domain and is coupled with the rest of the compressor mathematical models. They could not account for the exit pipe from the collector. This, however, was incorporated later on by Soedel in the form of a time domain model for the special case of an anechoic termination [9]. This technique was then extended to a four cylinder automotive compressor eigenvalue solution problem [10].

Schwerzler [11] modeled suction and discharge systems of a multicylinder compressor by using only a quasi-steady mean pressure variation technique in which he ignored coupling effects between cylinders. Wang [12] did not account for these interactions as he analyzed a multicylinder engine air induction system. In this investigation cylinders were considered in parallel, and sequential time relationships between them were modeled. Benson and Ucer [13] also do not consider multicylinder interactions in their method of characteristic technique. The literature search has not revealed any other investigation on the dynamic interactions between cylinders.

1.3. MODELING OBJECTIVES

Gas pulsations affect compressor capacity and energy requirements, valve motion and piping vibrations, and could even be a potential cause of the radiated noise. The locations at which the knowledge of pressure pulsations is important are as follows [14]:

(i) valve chamber: pulsating pressure in the valve chamber (p_v) affects cylinder capacity, power and valve displacement; the first few harmonics of the running speed are of fundamental significance;

(ii) manifold end: pulsating pressure at the end of the compressor discharge/suction system (p_a) indicates muffling effectiveness, and thus is a measure of fluid-borne noise transmitted to other components of the compression system.

Therefore, in general terms, the objective is to establish a computer simulation procedure as a design tool for multicylinder compressors with special emphasis on gas pulsations.

Specifically, the objectives of the present investigation are as follows: (i) define the multicylinder interaction problem; (ii) develop a modeling technique for multicylinder discharge (and similarly suction) systems; (iii) combine discharge models with compressor cylinder and valve models for inclusion of source characteristics, back pressure effect, etc.; and (iv) simplify compressor basic simulation models [5, 6, 15] without sacrificing any accuracy.

The aim of the study reported here is to model discharge systems with steady state acoustical impedances in the distributed parameter format. The impedance concept was first tried by Elson and Soedel [6] on a single cylinder compressor. They determined that it is more efficient and general than some classical approaches. The procedure is interactive in nature as it simulates the effect of discharge back pressure on the automatic valves. Elson and Soedel [6] tried it for a very simple system (a valve chamber connected to long

lines) and obtained good results. However, they could not generalize the procedure for a multicylinder case, and also did not show its applicability to complex practical configurations. In the study reported here such efforts were undertaken.

An upper frequency limit of 600 Hz was imposed, in the preliminary phase of the investigation, for the example case as the prediction of the first 10 harmonics for a 3600 rpm refrigeration compressor was considered adequate.

2. DISCHARGE SYSTEM MODEL

2.1. CYLINDER INTERACTIONS

The interactions can be thought of as consisting of two types of coupling: kinematic and geometric.

In respect to the kinematic coupling, the kinematic arrangement of a multicylinder reciprocating compressor is such that the instantaneous crank angles of all the cylinders are not the same. Thus, during a cycle, cylinders do not discharge simultaneously. The time lag between any two cylinders corresponds to their relative crank phasing. In the frequency domain, this time lag is considered as the phase lag (or lead), and should be accounted for with each and every harmonic.

In respect to the geometric coupling, the cylinders are generally connected to each other through passages and plenums. The mean fluid flow follows the pattern of these geometries and is pumped downstream. The acoustic waves not only propagate down the discharge line of one cylinder but also influence each other through the connecting elements. The impedance inequalities, all over the lines, reflect the acoustic waves back and forth. Thus, in a discharge system component there are incident and reflected waves corresponding to not only its respective cylinder but also to all the other cylinders. Hence, the resulting pressure in front of any discharge valve has components corresponding to not only its respective cylinder but also to all of the mass flow rates. Of course, the main component is due to its own mass flow rate input, and other cylinders may enhance or subdue it. Similarly, at any other point in the system, the waves from all the cylinders interfere with each other.

Kinematic coupling in the absence of geometric coupling will not cause any dynamic interactions between the cylinders. The only result will be that the discharge pressures of all the cylinders will have the same phase relationships amongst them as that of the rest of the compressor processes. On the other hand, the geometric coupling in the absence of kinematic coupling will cause fluid dynamic interactions. The waves, from all of the valve exits, will start simultaneously and propagate in the system, and dynamic interference will take place. When the kinematic coupling is superimposed on the geometric coupling, then the waves from the valve exits do not start simultaneously. Now the interference phenomenon is going to be rather complicated. One has to keep track of both the amplitude and phase of each and every harmonic of a cylinder. The similar harmonics (in-phase) cause a constructive interference and the dissimilar harmonics (out of phase) cause a destructive interference.

Thus, one can picture the multicylinder discharge case as a dynamic system with multiple periodic non-simultaneous input signals, the output being the unsteady fluid pressure which is influenced by subsystem interactions.

2.2. MATHEMATICAL FORMULATION

Consider the case of a generalized k cylinder compressor. From the crank and connecting rod arrangements, the phasing (ϕ) between the cylinders can be determined (a list of nomen-

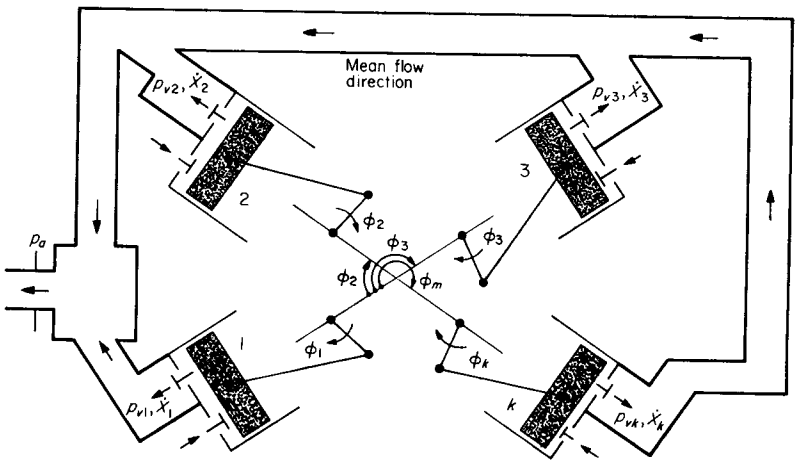

Figure 1. Schematic of a multicylinder compressor.

clature is given in the Appendix). For the schematic shown in Figure 1, the instantaneous crank angle (θ) for any cylinder, say i, is given as

$$\theta_i = \omega t + \phi_i, \qquad i = 1, 2, \ldots, k, \tag{1}$$

where ω is the running speed frequency in radians/second, t is the time and ϕ_i is the kinematic phasing relative to the first cylinder ($\phi_1 = 0$).

The source function, for the excitation of discharge gas oscillations, is the mass flow rate $(\dot{m}_i(t))_{\theta_i}$ through the discharge valve. As it is a periodic phenomenon, the Fourier series representation is

$$[\dot{m}_i(t)]_{\theta_i} = [\dot{m}_i(0) + \sum_{n=1}^{N} |\tilde{\dot{m}}_i(n\omega)| \exp j(n\omega t + \psi_{\dot{m}_i}(n\omega))]_{\theta_i}, \qquad i = 1, 2, \ldots, k, \tag{2}$$

where n is the number of the harmonic, N is the total number of harmonics, and the $\tilde{}$ sign over symbols implies that it is a complex quantity. The Fourier series representation has to take into account the instantaneous crank angle of each cylinder. The volume velocity $\tilde{X}(n\omega)$, a frequency domain concept, is defined for the ith cylinder as

$$[\tilde{\dot{X}}_i(n\omega)]_{\theta_i} = [\tilde{\dot{m}}_{v_i}(n\omega)]_{\theta_i}/\rho_i = |\tilde{\dot{X}}_i(n\omega)|_{\theta i} \exp\{j[n\omega t + \psi_{\dot{X}_i}(n\omega)_{\theta i}]\}, \qquad i = 1, 2, \ldots, k,$$
$$n = 0, 1, 2, \ldots, N, \tag{3}$$

where ρ is the fluid density.

Thus, the total number of volume velocity harmonics, required to describe the input completely, is equal to $k(N + 1)$. Each of the harmonic components is complex and has both magnitude and phase. Thus, the total number of terms is $2k(N + 1)$. For a symmetrical system, as all the cylinders have the same amount of discharge, the amplitudes of the volume velocities $\tilde{X}(n\omega)$ should be the same. It should be noted that the phases of the volume velocities may not be the same as kinematic phasing (ϕ_i) is involved. Thus, the total number of terms required would be $(k + 1)(N + 1)$.

The discharge pressure is given by the superposition of steady and unsteady components. The unsteady or pulsating pressure calculations problem is formulated in the following manner:

(i) make a pressure calculation at the valve exit of each cylinder (i.e., in the valve chamber); for example, the pressures $p_{v1}(t), p_{v2}(t), \ldots, p_{vk}(t)$ as shown in Figure 1;

(ii) make a pressure calculation at any intermediate point in the system; for example, the pressure $p_a(t)$ in the anechoic line, as shown in Figure 1.

2.2.1. *Valve chamber pressure* (p_{vi})

The source function, $\dot{m}_i(\theta_i)$, has already been converted to the frequency domain in the form of the volume velocity $[\tilde{\dot{X}}_i(n\omega)]_{\theta_i}$. A valve can now be replaced by a reciprocating piston which would provide a harmonic input of $[\tilde{\dot{X}}_i(n\omega)]_{\theta_i}$ to the discharge system. Thus, the discharge system is being excited at the frequency $n\omega$ by k harmonic volume velocity inputs. The acoustic wave oscillations will be created in the system at the excitation frequency. Consider cylinder 1; the pressure in front of the valve (or piston now) is $\tilde{p}_{v1}(n\omega)$. It has the contributions from all the cylinders. The pressure $\tilde{p}_{v1}(n\omega)$ can be related to all the volume velocities through the discharge system impedances which are defined as follows:

$$\text{input impedance: } \tilde{Z}_{qq}(n\omega) = \tilde{p}_q(n\omega)/\tilde{\dot{X}}_q(n\omega), \qquad q = 1, 2, \ldots, k, \tag{4}$$

$$\text{transfer impedance: } \tilde{Z}_{qr}(n\omega) = \tilde{p}_q(n\omega)/\tilde{\dot{X}}_r(n\omega), \qquad q \neq r, \quad r = 1, 2, \ldots k, \quad \text{and } q = 1, 2, \ldots, k. \tag{5}$$

Thus, $\tilde{p}_1(n\omega)$ can be written as

$$\tilde{p}_{v1}(n\omega) = \tilde{Z}_{11}(n\omega)[\tilde{\dot{X}}_1(n\omega)]_{\theta_1} + \tilde{Z}_{12}(n\omega)[\tilde{\dot{X}}_2(n\omega)]_{\theta_2} + \tilde{Z}_{13}(n\omega)[\tilde{\dot{X}}_3(n\omega)]_{\theta 3} + \ldots + \tilde{Z}_{1m}(n\omega)[\tilde{\dot{X}}_k(n\omega)]_{\theta k}, \tag{6}$$

where $\tilde{Z}_{11}(n\omega)$ is an input impedance term at the frequency $n\omega$ and $\tilde{Z}_{12}(n\omega), \tilde{Z}_{13}(n\omega), \ldots, \tilde{Z}_{1k}(n\omega)$ are the transfer impedance terms at the frequency $n\omega$.

Similar relationships can be written at other valve exits for $\tilde{p}_{v2}(n\omega), \tilde{p}_{v3}(n\omega), \ldots, \tilde{p}_{vm}(n\omega)$. In a generalized fashion, one has, for the ith cylinder valve exit,

$$\tilde{p}_{vi}(n\omega) = \sum_{q=1}^{k} \tilde{Z}_{iq}(n\omega)[\tilde{\dot{X}}_q(n\omega)]_{\theta_q}. \tag{7}$$

Thus, for a combined matrix format, the valve exit pressures are

$$\{\tilde{\boldsymbol{p}}_v(n\omega)\} = [\tilde{\mathbf{Z}}(n\omega)]_v\{[\tilde{\dot{\mathbf{X}}}(n\omega)]_{\theta_i}\}, \tag{8}$$

where $[\tilde{\mathbf{Z}}(n\omega)]_v$ is the valve impedance matrix (a square matrix).

The kinematic coupling has been accounted for in the volume velocity matrix. In the expression $\{[\tilde{\dot{\mathbf{X}}}(n\omega)]_{\theta_i}\}$, θ_i signifies that each volume velocity Fourier transform should be obtained at its respective value of the crank angle.

The impedance matrix $[\tilde{\mathbf{Z}}(n\omega)]_v$ has k^2 terms. Among these are k input and $k(k-1)$ transfer impedances. If the cavities were not interconnected, then there would be no fluid dynamic interaction between the various discharge lines, and each cylinder's discharge line pressure would depend only upon its own impedance. For such a case, the impedance matrix will be diagonal as transfer impedance terms will not exist. Thus, the transfer impedances account for the geometric coupling.

Since impedance is a complex quantity, the total number of impedance values required for the complete description is $2k^2$. This could be reduced by using the reciprocity relationship which holds good for all linear systems [16, 17]. It should be noted here that the discharge system will be analyzed by using linear acoustic theory, as this is considered adequate. However, the justification for this must ultimately be derived from the comparison of

theoretical results with analogous laboratory measurements. The reciprocity relationship is

$$\tilde{Z}_{qr} = \tilde{Z}_{rq}, \quad r \neq q. \tag{9}$$

Application of this relationship reduces the total number of impedance values required to $k(k + 1)$, and the total number of terms required for the pressure matrix computation to $k(k + 3)$.

Expression (8) provides the pressure only at a particular frequency. The total time dependent pressure $p(t)$ is

$$\{p_v(t)\}_v = \{\bar{p}_v\} + \{p_v(0)\}_v + \sum_{n=1}^{N} |\{\tilde{p}_v(n\omega)\}| \cos[(n\omega t) + \{\psi_{p_v}(n\omega)\}], \tag{10}$$

where $\{p_v(t)\}_v$ is the total pressure matrix (time dependent), $\{\bar{p}_v\}$ is the mean (static) pressure matrix, $\{p_v(0)\}$ is the d.c. (zero frequency component of the fluctuations) pressure matrix, $|\{\tilde{p}_v(n\omega)\}|$ is the harmonic pressure magnitude matrix and $\{\psi_{p_v}(n\omega)\}$ is the harmonic pressure phase; here $\{\tilde{p}_v(0)\}$, $|\{\tilde{p}(n\omega)\}|$, and $\{\psi_{p_v}(n\omega)\}$ are to be obtained from equation (8). The total number of values required for the computation of $\{p(t)\}$ is $k\{(k + 3)(N + 1) + 1\}$.

For a symmetrical multicylinder compressor discharge system, the amount of information needed would be drastically reduced. However, it cannot be generalized as it depends strictly on the system geometry. For example, in some symmetrical cases, only one input impedance, one transfer impedance, and one volume velocity term (for a particular frequency) may be needed.

2.2.2. *Anechoic line pressure* (p_a)

The anechoic line pressure will have contributions from each cylinder, in accordance with

$$\tilde{p}_a(n\omega) = [\tilde{Z}_{a1}(n\omega)\tilde{Z}_{a2}(n\omega) \ldots \tilde{Z}_{ak}(n\omega)] \begin{Bmatrix} [\tilde{X}_1(n\omega)]_{\theta_1} \\ [\tilde{X}_2(n\omega)]_{\theta_2} \\ \vdots \\ [\tilde{X}_k(n\omega)]_{\theta_k} \end{Bmatrix}, \tag{11a}$$

or

$$\tilde{p}_a(n\omega) = [\tilde{\mathbf{Z}}(n\omega)]_a \{[\tilde{\mathbf{X}}(n\omega)]_{\theta_i}\}, \tag{11b}$$

where $[\tilde{\mathbf{Z}}(n\omega)]_a$ is the anechoic impedance matrix (a row matrix). It should be noted here that the transfer impedance formulation applies to any point in the system except valve exits. However, the impedance terms would not be the same for two points, and they have to be evaluated separately for each point. The impedance matrix $[\tilde{\mathbf{Z}}]_a$ has only the transfer impedance term as there are no input impedance terms. For an uncoupled system, only one transfer impedance term would exist for a point, and it would correspond to that particular cylinder. The total information required for the transfer impedance matrix description is $2k$ values.

The time dependent total pressure $p_a(t)$ is similar to that given in equation (10):

$$p_a(t) = \bar{p}_a + p_a(0) + \sum_{n=1}^{N} |\tilde{p}_a(n\omega)| \cos[n\omega t + \psi_{p_a}(n\omega)]. \tag{12}$$

The total information required for $p_a(t)$ is $k(4N + 5)$ values. Again, for a symmetrical system this could be reduced drastically.

Both $[\tilde{\mathbf{Z}}(n\omega)]_v$ and $[\tilde{\mathbf{Z}}(n\omega)]_a$ could also be combined into a single matrix.

2.3. IMPEDANCE COMPUTATIONS

Acoustic impedances are inherent system characteristics, and are uniquely related to the geometry and fluid medium [16, 17]. Consider a discharge system element with unknown impedances, as shown in Figure 2, where the input (q) and output (r) variables are related

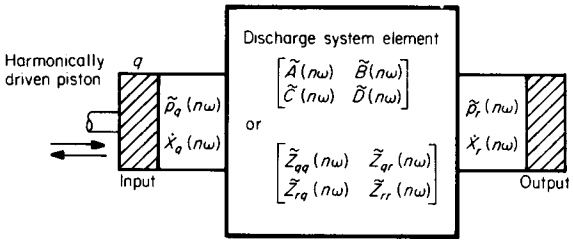

Figure 2. Relationship between input and output variables of a discharge system element.

through the system characteristics. For a steady state harmonic excitation of radian frequency ω,

$$\begin{Bmatrix} \tilde{p}_q(\omega) \\ \tilde{p}_r(\omega) \end{Bmatrix} = \begin{bmatrix} \tilde{Z}_{qq}(\omega)\ \tilde{Z}_{qr}(\omega) \\ \tilde{Z}_{rq}(\omega)\ \tilde{Z}_{rr}(\omega) \end{bmatrix} \begin{Bmatrix} \tilde{\dot{X}}_q(\omega) \\ \tilde{\dot{X}}_r(\omega) \end{Bmatrix}. \tag{13}$$

A relationship between input and output variables can also be expressed through a four-pole formulation:

$$\begin{Bmatrix} \tilde{p}_q(\omega) \\ \tilde{\dot{X}}_q(\omega) \end{Bmatrix} = \begin{bmatrix} \tilde{A}(\omega) & \tilde{B}(\omega) \\ \tilde{C}(\omega) & \tilde{D}(\omega) \end{bmatrix} \begin{Bmatrix} \tilde{p}_r(\omega) \\ \tilde{\dot{X}}_r(\omega) \end{Bmatrix}. \tag{14}$$

The four-pole coefficients are also fundamental properties of an acoustic system, and are thus related to the impedance components. Using the four-pole properties and reciprocity relationship, one obtains

$$\tilde{A}(\omega) = \tilde{Z}_{qq}(\omega)/\tilde{Z}_{qr}(\omega), \tag{15}$$

$$\tilde{B}(\omega) = [\tilde{Z}_{qq}(\omega)\,\tilde{Z}_{rr}(\omega) - \tilde{Z}^2_{qr}(\omega)]/\tilde{Z}_{qr}(\omega), \tag{16}$$

$$\tilde{C}(\omega) = 1/\tilde{Z}_{qr}(\omega), \tag{17}$$

$$\tilde{D}(\omega) = \tilde{Z}_{rr}(\omega)/\tilde{Z}_{qr}(\omega). \tag{18}$$

Thus an impedance matrix can be easily transformed into a four-pole matrix and vice versa. In general it is easy to work with a four-pole type of transfer matrix because of the simple algebraic operations and building block type of approach [18, 19].

To compute input and transfer impedance matrices, the following approach can be followed; (i) consider any two points, say q and r, in the discharge and formulate the problem in terms of impedances; (ii) develop the four-pole relationship between q and r; (iii) compute impedance matrix terms by using equations (15) through (18).

2.4. EXAMPLE CASE: DISCHARGE SYSTEM

Figure 3 shows schematically the example case: the discharge system of a two cylinder reciprocating compressor. The discharge system consists of manifolds in the cylinder head and the associated muffling arrangement.

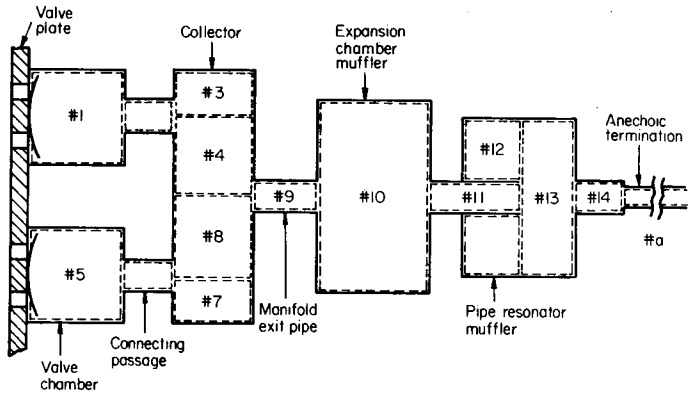

Figure 3. Example case: schematic of a two cylinder reciprocating compressor discharge system.

The assumptions for analyzing this example case are as follows.

1. The fluid medium is considered homogeneous, continuous, isotropic and perfectly elastic. An adiabatic process is assumed and the side walls are considered rigid and non-heat conducting.
2. The theory of small pressure oscillations is assumed to hold good. Only plane wave propagation is considered. This assumption is valid as the largest transverse dimension is small compared to the smallest sound wave-length of interest.
3. All discontinuities are abrupt and there is no sound diffraction. The disturbing influence of any element is assumed to be very small and confined to a small region (as compared to the wave-length). However, in some cases the additional kinetic energy is accounted for through standard end corrections [16, 17].
4. The sound waves are considered to be following the wave guide. A curved or bent tube is considered a straight tube of length corresponding to the median length of the actual element. This assumption is valid for plane waves and large bends.
5. The convective effect of the steady fluid flow is ignored as the maximum flow velocities are less than Mach 0·1. However, the fluid induced damping effects are considered [17, 20].
6. The discharge system end is considered to be anechoic: i.e., no acoustic energy is reflected back. In fact, refrigeration compressors are usually evaluated for pressure pulsations with an anechoic termination as it isolates the compressor discharge system from the dynamic effects of the rest of the refrigeration system.

Acoustical transmission line theory in terms of distributed parameters is used here to describe the example case. Since it has all tubular elements, one needs only the four-pole matrix of a finite tube of circular cross-sectional area S and length l [16]: namely,

$$\tilde{A}_q = \begin{bmatrix} \tilde{A}_q & \tilde{B}_q \\ \tilde{C}_q & \tilde{D}_q \end{bmatrix} = \begin{bmatrix} \cosh \tilde{\gamma}_q l_q & (\rho c/S_q) \sinh \tilde{\gamma}_q l_q \\ (S_q/\rho c) \sinh \tilde{\gamma}_q l_q & \cosh \tilde{\gamma}_q l_q \end{bmatrix}, \tag{19a}$$

where γ is the propagation constant,

$$\tilde{\gamma}_q = \beta_q + \mathrm{j}\,\omega/c \tag{19b}$$

where β is the damping factor.

In expression (17), l represents the effective length, which includes the effect of attached mass (only in the inertial elements): i.e.,

$$l = (l)_{\text{geometric}} + \sigma, \tag{20}$$

where σ is the end correction, which needs to be applied to each end ($\sigma = 0{\cdot}32d$ for an unflanged end, and $\sigma = 0{\cdot}425d$ for a flanged end, where d is the diameter [17]).

For analysis purposes, the discharge system as shown in Figure 3 has been divided into various acoustical elements which are assigned identification numbers. The impedance formulation is as follows:

$$\tilde{Z}_{11} = \tilde{A}_{1,5}/\tilde{C}_{1,5}, \qquad \tilde{Z}_{15} = \tilde{Z}_{51} = 1/\tilde{C}_{1,5}, \qquad \tilde{Z}_{55} = \tilde{D}_{1,5}/\tilde{C}_{1,5}, \tag{21–23}$$

$$\tilde{Z}_{a1} = 1/\tilde{C}_{1,a}, \qquad \tilde{Z}_{a5} = 1/\tilde{C}_{5,a}. \tag{24, 25}$$

The four-pole coefficients are given by the following:

$$\begin{bmatrix} \tilde{A}_{1,5} & \tilde{B}_{1,5} \\ \tilde{C}_{1,5} & \tilde{D}_{1,5} \end{bmatrix} = \tilde{\Delta}_1 \cdot \tilde{\Delta}_2 \cdot \tilde{\mathbf{F}}_3 \cdot \tilde{\Delta}_4 \cdot \tilde{\mathbf{F}}_b \cdot \tilde{\Delta}_8 \cdot \tilde{\mathbf{F}}_7 \cdot \tilde{\Delta}_6 \cdot \tilde{\Delta}_5, \tag{26}$$

$$\begin{bmatrix} \tilde{A}_{1,a} & \tilde{B}_{1,a} \\ \tilde{C}_{1,a} & \tilde{D}_{1,a} \end{bmatrix} = \tilde{\Delta}_1 \cdot \tilde{\Delta}_2 \cdot \tilde{\mathbf{F}}_3 \cdot \tilde{\Delta}_4 \cdot \tilde{\mathbf{F}}_{II} \cdot \tilde{\mathbf{F}}_e, \qquad \begin{bmatrix} \tilde{A}_{5,a} & \tilde{B}_{5,a} \\ \tilde{C}_{5,a} & \tilde{D}_{5,a} \end{bmatrix} = \tilde{\Delta}_5 \cdot \tilde{\Delta}_6 \cdot \tilde{\mathbf{F}}_7 \cdot \tilde{\Delta}_8 \cdot \tilde{\mathbf{F}}_I \cdot \tilde{\mathbf{F}}_e, \tag{27, 28}$$

where $\tilde{\mathbf{F}}_3$, $\tilde{\mathbf{F}}_7$ and $\tilde{\mathbf{F}}_b$ are

$$\tilde{\mathbf{F}}_3 = \begin{bmatrix} 1 & 0 \\ (S_3/\rho c)\tanh \tilde{\gamma}_3 l_3 & 1 \end{bmatrix}, \qquad \tilde{\mathbf{F}}_7 = \begin{bmatrix} 1 & 0 \\ (S_7/\rho c)\tanh \tilde{\gamma}_7 l_7 & 1 \end{bmatrix},$$

$$\tilde{\mathbf{F}}_b = \begin{bmatrix} 1 & 0 \\ \tilde{C}_e/A_e & 1 \end{bmatrix}, \tag{29–31}$$

$\tilde{\mathbf{F}}_e$ is given by

$$\tilde{\mathbf{F}}_e = \begin{bmatrix} \tilde{A}_e & \tilde{B}_e \\ \tilde{C}_e & \tilde{D}_e \end{bmatrix} = \tilde{\Delta}_9 \cdot \tilde{\Delta}_{10} \cdot \tilde{\Delta}_{11} \cdot \tilde{\mathbf{F}}_{12} \cdot \tilde{\Delta}_{13} \cdot \tilde{\Delta}_{14} \cdot \tilde{\mathbf{F}}_a, \tag{32}$$

where $\tilde{\mathbf{F}}_{12}$ and $\tilde{\mathbf{F}}_a$ are

$$\tilde{\mathbf{F}}_{12} = \begin{bmatrix} 1 & 0 \\ (S_{12}/\rho c)\tanh \tilde{\gamma}_{12} l_{12} & 1 \end{bmatrix}, \qquad \tilde{\mathbf{F}}_a = \begin{bmatrix} 1 & 0 \\ S_a/\rho c & 1 \end{bmatrix}, \tag{33, 34}$$

and $\tilde{\mathbf{F}}_{II}$ and $\tilde{\mathbf{F}}_I$ are

$$\tilde{\mathbf{F}}_{II} = \tilde{\Delta}_8 \cdot \tilde{\mathbf{F}}_7 \cdot \tilde{\Delta}_6 \cdot \tilde{\Delta}_5, \qquad \tilde{\mathbf{F}}_I = \tilde{\Delta}_4 \cdot \tilde{\mathbf{F}}_3 \cdot \tilde{\Delta}_2 \cdot \tilde{\Delta}_1. \tag{35, 36}$$

3. COMPRESSOR SIMULATION

3.1. BASIC MATHEMATICAL MODELS

The computer simulation model describes the basic operation of the compressor and predicts operating variables on an instantaneous basis. Since the compressor processes are cyclic in nature, mathematical models are converted from the time domain to the θ domain by using equation (1).

A general documentation of the cylinder and valve simulation equations for the multicylinder case is available in references [5] and [21–23]. Since the present investigation

focuses on the elaborate simulation of discharge line pressures, basic compressor models have been simplified. Theoretical engineering approximations instead of usual experimental inputs, and the results of other investigations, have been incorporated into the total compressor simulation model which comprises the following.

1. *Cylinder models.* The equation of state, the energy equation, the continuity equation and a kinematics model are required to predict the instantaneous cylinder variables: e.g., pressure, temperature, density and volume.
2. *Discharge valve models.* Because of the strong dynamic interaction between the discharge line and valve, special attention has been given to the valve modeling, especially mass flow rate prediction. The valve models consist of the following: (a) fluid dynamics – for the mass flow rate prediction, and (b) structural dynamics – for the instantaneous valve displacement. The structural model of the ring type valves has been simplified to the point where it no longer describes the wrapping of the valve reed around the stop [6, 15], but it still predicts mass flow rate adequately. Note here that the valve motion is now predicted by using a single mode approximation which is compatible with the upper frequency limitation dictated by the pulsations. The assumption of single mode approximation is valid because the first mode is dominant.
3. *Suction valve models.* Modeling of a suction valve is similar to that for the discharge valve.
4. *Suction line model.* Suction conditions are considered steady and non-oscillatory. This assumption is valid as suction pulsations are very low.

The validity of the simplifications is evaluated by comparing the present simple valve model with the elaborate valve modelling efforts of Elson and Soedel [6]. The results are compared in Figure 4 for a single cylinder example case presented in reference [6]. Since the discharge pressure results compare very well, the validity of the accuracy of mass flow rate prediction by using the simple model is established.

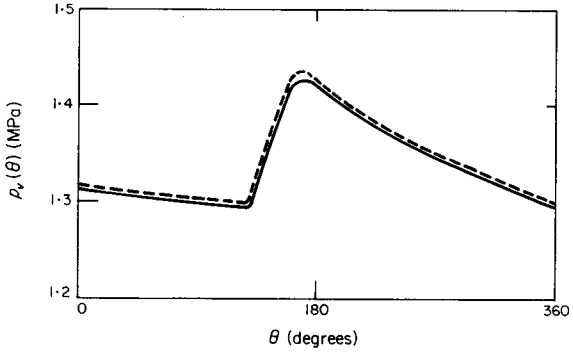

Figure 4. Illustration of the validity of discharge valve modeling simplification. Cyclic pressure variation $p_v(\theta)$ in a single cylinder discharge chamber, with elaborate valve modeling ———, and with present simplified valve modeling – – – –.

3.2. MASS FLOW RATE PREDICTION

Discharge valve mass flow rate data is converted to the frequency domain in order to evaluate the volume velocity data. Since the simulation provides mass flow rate data at discrete points, a finite Fourier series formulation is required. The terms in equation (2) are computed as follows:

$$|\dot{m}_i(n\omega)|_{\theta_i} = (a_{ni}^2 + b_{ni}^2)^{1/2}, \qquad \psi_{\dot{m}_i}(n\omega)_{\theta_i} = -\arctan(b_{ni}/a_{ni}) \qquad (37, 38)$$

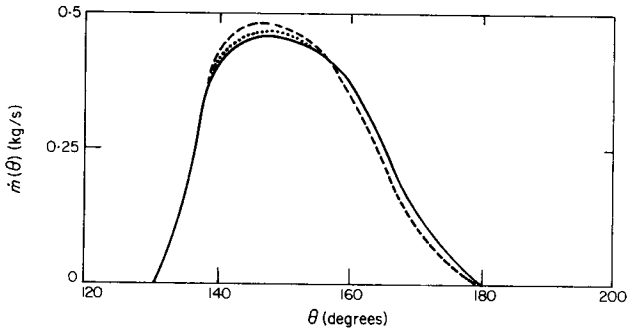

Figure 5. Effect of the crank angle resolution ($\delta\theta$) in computations on the simulated mass flow rate through the discharge valve, $\dot{m}(\theta)$. $\delta\theta = 1°$ ——; $\delta\theta = \frac{1}{2}°$ .....; $\delta\theta = 1°/10, 1°/50, 1°/100$ and $1°/500$ ———.

where the a_{ni} and b_{ni} are given by

$$a_{ni} = \frac{2}{M} \sum_{\alpha=0}^{M} \dot{m}_i(\theta_\alpha) \cos n\theta_\alpha, \qquad n = 0, 1, \ldots, N, \tag{39}$$

$$b_{ni} = \frac{2}{M} \sum_{\alpha=0}^{M} \dot{m}_1(\theta_\alpha) \sin n\theta_\alpha, \qquad n = 0, 1, \ldots, N, \tag{40}$$

where M is the total number of sampling points and is given in terms of the crank angle resolution $\delta\theta$, in degrees, as $M\delta\theta = 360$. By comparing mass flow rates, $\delta\theta$ is optimized, as shown in Figure 5. It is taken as $1/2°$, as a step size lower than this does not have any effect on accuracy. It should be noted that $\delta\theta$ is also a strong function of valve natural frequencies.

For the conversion of mass flow rate data from the time (or θ) domain to the frequency domain and *vice versa*, one needs to have almost an infinite number of harmonic terms (N), and even then some information is always lost in the conversion. Figure 6 shows the comparison between the original mass flow rate data and the recreated mass flow data through a harmonic analysis with $N = 20$. The slight oscillatory condition of the recreated data is due to the fact that the first 20 terms are not enough to provide an exact representation. Here, it should be noted that taking N equal to only 20 does not mean that it is inaccurate or that the higher frequencies are thrown away. Above this frequency, the mass flow rate

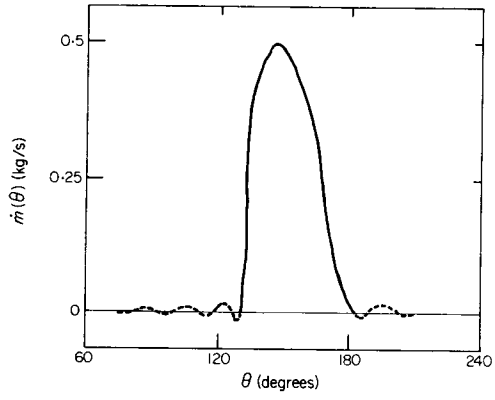

Figure 6. Comparison between simulated discharge mass flow rate ——— and the recreated mass flow rate (as obtained by using the first 29 harmonics of the simulated data – – – –.

data is probably inaccurate because of the simplifications in valve dynamics. Also, discharge system impedances will not be computed above this frequency because of the plane wave consideration.

3.3. COMPUTATIONAL SCHEME

To account for the back pressure effect, the following iterative computational procedure is utilized.

1. To start the simulation program, set $p(\theta) = \bar{p}$ (see equations (10) and (12), and note that $p(\theta) = p(t)$). If $\bar{p}$ is not known, assume a suitable value. The program will correct this initial condition after a few iterations.
2. Initiate simulation at $\theta_1 = 0$: i.e., at the bottom dead center of the cylinder 1. Increment the program at $\delta\theta$ and predict basic operating variables for each cylinder.
3. Store the $\dot{m}_i(\theta)$ data for a cycle, and convert this into harmonic data by using Fourier transforms (37) to (40). Compute the volume velocity matrix $\{[\tilde{X}(n\omega)]_{\theta_i}\}$ by using equation (3).
4. Compute the harmonic pressures $\{\tilde{p}_v(n\omega)\}$ and $\tilde{p}_d(n\omega)$ by using equations (8) and (11). Check the convergence of each harmonic. If harmonics have converged, stop iteration after step 5, and otherwise return to the simulation program with discharge pressures computed in step 5.
5. Compute the cyclic pressures $\{p_v(\theta)\}$ and $p_d(\theta)$ by using inverse Fourier transforms (10) and (12).

The convergence of the simulation program is quite fast as demonstrated in Figure 7. Although only three iterations are sufficient for fairly good results, eight iterations have been employed to get the final results.

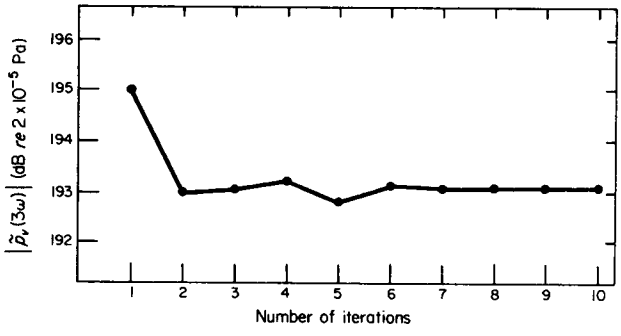

Figure 7. Typical convergence pattern of pressure harmonics, as shown above for a third harmonic of the valve chamber pressure, $|\tilde{p}_v(3\omega)|$.

3.4. EXAMPLE CASE: TWO CYLINDER COMPRESSOR

The example case with the instrumentation is shown schematically in Figure 8. It is an in-line type of high speed reciprocating compressor with the following specifications: $k = 2$, $\phi = 180°$, fluid medium the refrigerant R-12 (CCl_2F_2), bore = 51 mm, stroke = 29 mm, running speed = 59·66 Hz (ω = 374·9 rad/s). The discharge system as shown in Figure 3 is installed here. It is symmetrical for both cylinders (i.e., in Figure 3 elements 1 = 5, 3 = 7, 4 = 8). The anechoic termination is achieved by employing a 15 m long copper

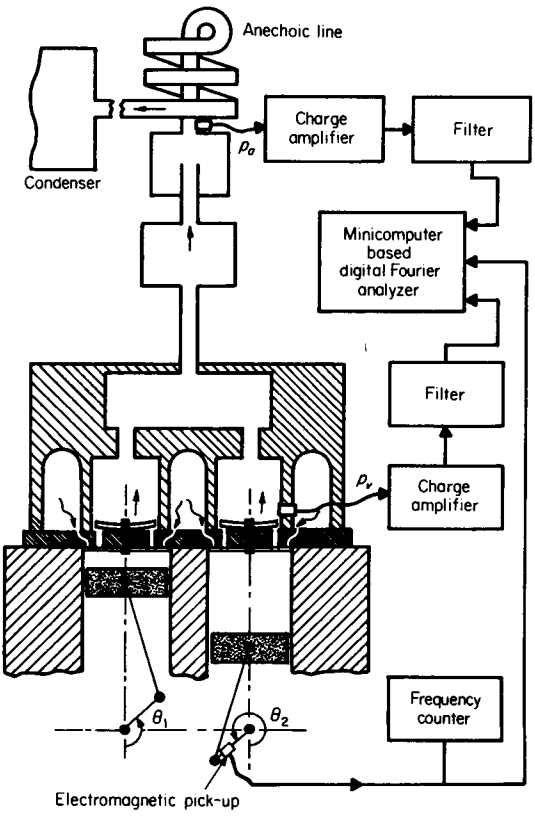

Figure 8. Example case with instrumentation.

tubing (inner diameter = 11 mm) in between discharge system and condenser coils. Although for the no flow situation this length may not be sufficient, mean fluid flow laden with oil vapors provides substantial attenuation. Still, reflections can result from coil bends and other geometric discontinuities. Thus this termination can not be considered truly anechoic, especially at lower frequencies, but it is adequate.

Two piezoelectric type dynamic pressure transducers are installed in the discharge system to measure the following: (i) $|\tilde{p}_v(n\omega)|$ and $p_v(\theta)$; note that with reference to Figure 3, $p_v = p_1, p_5$; and (ii) $|\tilde{p}_a(n\omega)|$ and $p_a(\theta)$. A 60 tooth gear with an electromagnetic pick-up is mounted on the crankshaft to establish the crank angle (θ) position. A minicomputer based digital system with a Fast Fourier Transform capability has been utilized for data acquisition and processing.

Uncertainties in the measurements are mainly due to (a) transducer sensitivities, (b) digital data processing procedures [24], and (c) the semi-anechoic nature of the termination at the first few harmonics. The experimental data for the present case have the following uncertainty (ε) values: $\varepsilon p(\theta) = \pm 5\%$; $\varepsilon|\tilde{p}(n\omega)| = \pm 1$ dB; $\varepsilon\theta = \pm 1°$.

4. RESULTS

Impedance computations are compared to the experimentally measured impedances in Figures 9 and 10 for a symmetrical discharge system (i.e., $\tilde{Z}_{11} = \tilde{Z}_{55}$ and $\tilde{Z}_{al} = \tilde{Z}_{51}$;

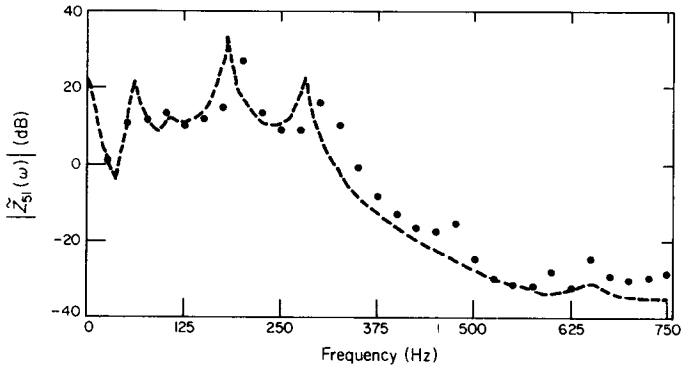

Figure 9. Dimensionless impedance magnitude, $|\tilde{z}_{51}(\omega)|$. Computed, ------; measured,○.

see section 2.4 and Figure 3). These plots are for an R-12 medium at room temperature and pressure (see reference [25] for the impedance measurement technique). Figure 9 shows the transfer impedance magnitude $\tilde{Z}_{51}$ in the dimensionless form as $20 \log_{10} |\tilde{Z}_{51}/(\rho c/S_1)|$. Figure 10 presents the input impedance phase $\psi_{Z_{11}}$ spectrum. The results show excellent agreement between theory and experiment with deviations resulting mainly from the measurement inadequacies.

An analysis of the impedance spectra reveals that in all there are four natural frequencies of gas oscillations: 70 Hz, 100 Hz, 190 Hz and 285 Hz. 70 and 100 Hz modes correspond to the single cylinder elements: i.e., 1–4 and 9–a in Figure 3. This can be achieved by blocking off the components (5–8) belonging to the other cylinder. Conversely, if the attention is focused only on the inner cavities, i.e., 1–8, then the gas oscillations produce 190 and 285 Hz modes. These result due to the geometric coupling between the cylinders. Out of all these four modes, the 190 Hz is the most dominant and 100 Hz is the weakest.

The cyclic pressure and spectral pressure results are presented in Figures 11–14, for the following operating conditions: nominal suction pressure = 0·28 MPa; nominal suction temperature = 16°C; nominal discharge pressure = 1·26 MPa; nominal discharge temperature = 73°C.

Figure 11 shows the valve chamber pressure magnitude frequency spectrum. It is in the form of the sound pressure level $(20 \log_{10} |\tilde{p}_v(n\omega)/p_{\text{ref}}|$, where $p_{\text{ref}} = 2 \times 10^{-5}$ Pa). Theory and experiment correlate very well over the entire frequency range of interest: i.e., over the first 20 harmonics. A closer examination of the results show that the third

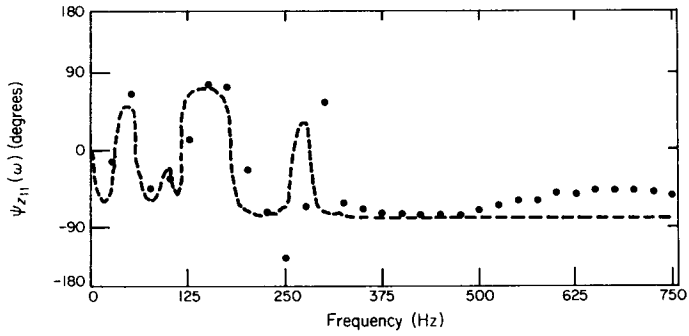

Figure 10. Impedance phase $\psi_{z_{11}}(\omega)$. Computed, ------; measured,○.

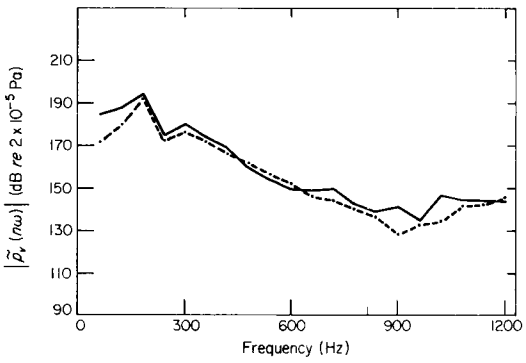

Figure 11. Spectral pressure in the discharge plenum, $|\tilde{p}_v(n\omega)|$, at the harmonics of 59·66 Hz. Computed, ----; measured, ———.

harmonic (180 Hz) is the most dominant. This results from the 190 Hz resonance. The 285 Hz resonance effect is not visible at all, because the kinematic coupling ($\phi = 180°$) is such that only one mode (190 Hz) is excited. Suppose that $\phi = 0°$; then only the 285 Hz resonance would be excited, and one would witness a fifth harmonic (300 Hz) dominance. For intermediate ϕ, both 190 and 285 Hz resonance effects should be seen. Note that the kinematic coupling affects only those modes which arise because of the geometric coupling.

The valve chamber cyclic pressure variation $p_v(\theta)$ is shown in Figure 12. It shows that three cycles of gas pulsations take place during one cycle of compressor operation. The maximum pressure is at the time of discharge valve opening ($\theta = 140°$–$190°$). Computed and measured results match very well. Of course, the prediction of time domain pressure depends very strongly on the accurate prediction of the most dominant harmonic, especially a lower one.

The computed anechoic line spectral pressure, $|\tilde{p}_a(n\omega)|$, is compared with the measured values in Figure 13. The agreement is very good considering the fact that discrepancy between computed and measured results could be due to the measurement of $|\tilde{p}_a(n\omega)|$. This signal was almost buried in flow noise (random in nature), and only an ensemble frequency domain averaging operation could unearth these very low level signals. Note here that the dynamic range of the computed spectrum is greater than the instrumentation range (60–70 dB) and that is why beyond 600 Hz the measured values simply reflect the

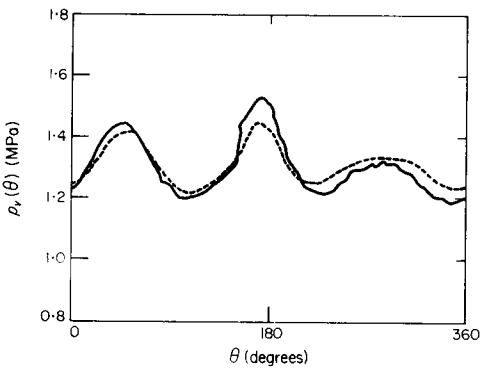

Figure 12. Cyclic pressure in the valve chamber, $p_v(\theta)$. Computed, -----; measured, ———. 180° is top dead center.

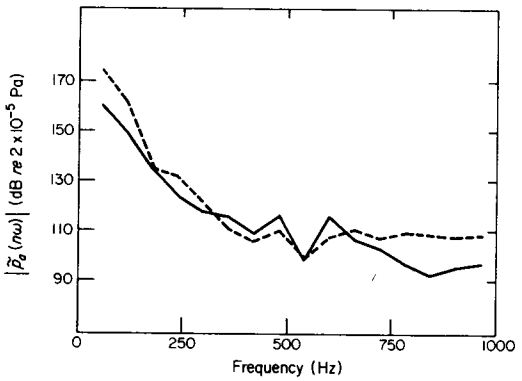

Figure 13. Spectral pressure in the anechoic line, $|\tilde{p}_a(n\omega)|$, at the harmonics of 59·66 Hz. Computed, ------; measured, ———.

noise floor of the instrumentation. However, the comparisons have been made up to 900 Hz.

Figure 13 clearly demonstrates the effectiveness of the manifold and muffler system. The first harmonic is virtually unchanged but the second harmonic is 20 dB down, and the rest of the harmonics have been attenuated by at least 40 dB. Thus, only the first two pressure harmonics are transmitted with significant levels. The reason may be two-fold: (i) the muffling system is essentially a low pass filter type, and (ii) single cylinder resonance effects (70 and 120 Hz), especially the 70 Hz resonance, could have a higher modal participation. The third harmonic is not visible as the 190 Hz mode seems to be the type of mode which results in no pressure fluctuations in the collecter (3, 4, 5 and 6 elements in Figure 3). This is because of the kinematic coupling arrangement ($\phi = 180°$). Thus, the third harmonic is not propagated downstream.

Peak to peak variation in anechoic line pressure $p_a(\theta)$ is generally regarded as a measure of fluid-borne noise transmitted to other components such as condenser/evaporator coils. Figure 14 presents this result. Both theory and measurement show a very small variation in pressure as compared to the mean operating pressure. Judging from the above-mentioned objective, the magnitude comparison can be termed excellent, but no definite comparison can be drawn for the phase, which is not relevant at this location.

Although a limit on the upper frequency prediction was placed at around 600 Hz, the results have been shown for 1200 Hz (except 900 Hz in the case of $|\tilde{p}_a(n\omega)|$). This is still within the plane wave propagation region as the first cut-off mode for the largest transverse dimen-

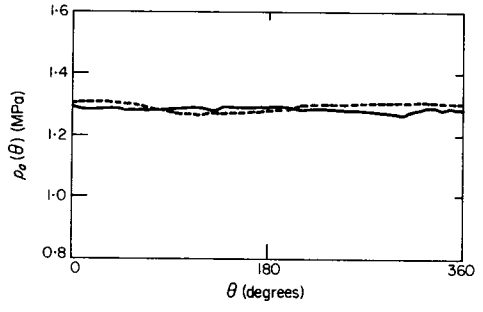

Figure 14. Cyclic pressure in the anechoic line, $p_a(\theta)$. Computed, ------; measured, ———. 180° is the top dead center.

sion in the example case is around 1350 Hz. Because of the sharp cut-off and eventual decay of higher modes, it is felt that the plane wave impedance formulation is adequate even for frequencies higher than 1350 Hz (provided the basic simulation model is compatible for this frequency region).

5. CONCLUDING REMARKS

The major accomplishment of the work described in this paper has been the definition and modeling of multicylinder interference mechanisms in compressor discharge systems. Discharge models are coupled with the cylinder and valve mathematical models, and thus back reaction of unsteady flows has been accounted for. Also, the steady state acoustic impedance function approach has been established as a sound solution technique. The transfer function approach of modeling discharge system components makes the overall simulation model attractive as a discharge component can be easily inserted or deleted. In spite of the modeling simplifications and emphasis on computational ease, precise pressure predictions have been achieved.

Perhaps of more fundamental importance has been the question of using linear acoustic theories for such complicated unsteady flow processes. The answer to this certainly lies in the excellent agreement between theoretical and experimental results. In compressor design/development work, it is important to predict the following: (a) conditions at which resonances occur so that these can be avoided and, (b) estimations of energy and pressure fluctuations at non-resonant conditions. Thus, precise predictions of non-linear phenomena such as finite amplitude can only be considered academic. In this context, we consider that the linear acoustics modeling philosophy is indeed adequate for most cases. However, for special cases one may have to incorporate individual non-linear effects into the easily analyzable formulations, with or without the aid of experiments.

Although the modeling procedure is presented here only for multicylinder compressor discharge systems, it is equally applicable to suction systems as well. Moreover, the authors see no reason why this technique cannot be readily extended to any multicylinder/inter-staged positive displacement fluid machine.

The investigation has mainly concentrated on the prediction of primary output such as gas pressures. The following secondary outputs can be related to and generated from the primary outputs: capacity, volumetric efficiency, performance, pulsations and vibration levels and stresses, etc. It is currently being used as a tool for design and optimization studies.

ACKNOWLEDGMENTS

The work reported here was sponsored by the Carlyle Compressor Company, Carrier Corporation, Syracuse, New York. The authors thank P. Baade, K. Barrows, T. Carter, T. Katra and F. Scheideman of Carrier Corporation for their assistance. The authors also wish to acknowledge E. Sandgren and K. Ragsdell of Purdue University for their considerable contribution to the computational phase of the example case.

REFERENCES

1. J. BRABLIK 1972 *Proceedings of the 1st Purdue Compressor Technology Conference*, 188–195. Gas pulsations affecting operation of automatic valves in reciprocating compressors.

2. J. F. T. McLaren and A. B. Tramschek 1972 *Proceedings of the 1st Purdue Compressor Technology Conference*, 203–211. Prediction of valve behaviour with pulsating flow in reciprocating compressors.
3. S. Touber and E. C. Blosnsana 1971 *Proceedings of the 13th International Congress of Refrigeration, Washington*, 595–605. Theoretical and experimental investigation of valve movement and instationary gas flow in a reciprocating compressor.
4. R. S. Benson and A. S. Ucer 1972 *Journal of Mechanical Engineering Science* **14**, 264–279. A theoretical and experimental investigation of a gas dynamic model for a single stage reciprocating compressor with intake and delivery pipe system.
5. W. Soedel, E. Padilla and B. D. Kotalik 1973 *Journal of Sound and Vibration* **30**, 263–277. On Helmholtz resonator effects in the discharge system of a two-cylinder compressor.
6. J. P. Elson and W. Soedel 1974 *Journal of Sound and Vibration* **34**, 211–220. Simulation of the interaction of the compressor valves with acoustic back pressures in long discharge lines.
7. R. Singh and W. Soedel 1974 *Proceedings of the 2nd Purdue Compressor Technology Conference*, 102–123. A review of compressor lines pulsation analysis and muffler design research, Part I: Pulsation effects and muffler criteria and Part II: Analysis of pulsating effects.
8. R. Singh and W. Soedel 1975 *International Institute of Refrigeration, Congress of Refrigeration, Moscow, Paper No. B2.15*. Simulation of compressor lines gas pulsations.
9. W. Soedel 1972 *Proceedings of the 2nd Purdue Compressor Technology Conference*, 136–139. On the simulation of anechoic pipes Helmholtz resonator models of compressor discharge systems.
10. W. Soedel and J. M. Baum 1976 *Proceedings of the 3rd Purdue Compressor Technology Conference*, 257–270. Natural frequencies and modes of gases in multicylinder compressor manifolds and their use in design.
11. D. Schwerzler 1971 *Ph.D. Thesis, Purdue University*. Mathematical modeling of multiple cylinder refrigeration compressor.
12. W. M. Wang 1967 *Journal of the Acoustical Society of America* **42**, 1244–1249. Acoustical analysis of a multicylinder engine air-induction system.
13. R. S. Benson and A. S. Ucer 1973 *Journal of Mechanical Engineering Science* **15**, 34–37. A theoretical pulsation in pipe systems with multiple reciprocating air compressors and receivers.
14. W. W. Nimitz 1974 *Proceedings of the 2nd Purdue Compressor Technology Conference*, 329–346. Reliability and performance assurance in the design of reciprocating compressor installations, Part I: Design criteria, Part II: Design technology.
15. J. P. Elson, W. Soedel and R. Cohen 1976 *Journal of Engineering for Industry, ASME Paper No. 75-DET-26*. A general method of simulating the flow dependent nonlinear vibrations of compressor reed valves.
16. S. N. Rschevkin 1963 *A Course of Lectures on the Theory of Sound*. New York: McMillan Company.
17. P. M. Morse and K. U. Ingard 1968 *Theoretical Acoustics*. New York: McGraw-Hill Book Company.
18. J. Igarashi and M. Toyama 1958 *University of Tokyo Aeronautical Research Institute*, 339. Fundamentals of acoustic silencers (I) Theory and experiment of acoustic low pass filters.
19. T. Miwa and J. Igarashi 1959 *University of Tokyo Aeronautical Research Institute*, 344, 25(4). Fundamentals of acoustic silencers (II) Determination of four terminal constants of acoustic elements.
20. R. Singh and W. Soedel 1978 *Journal of Sound and Vibration* **57**, 449–452. Assessment of fluid induced damping in refrigeration machinery manifolds.
21. E. Sandgren 1974 *MSME Thesis, Purdue University*. Computer simulation of a two-cylinder reciprocating compressor and associated discharge system using acoustical impedances.
22. R. Singh 1975 *Ph.D. Thesis, Purdue University*. Modeling of multicylinder compressor discharge systems.
23. R. Singh, E. Sandgren, K. Ragsdell and W. Soedel 1976 *American Society of Mechanical Engineers Winter Annual Meeting, ASME Paper No. 76-WA/FR-10*. Simulation of a two cylinder compressor for discharge gas oscillation prediction.
24. J. S. Bendat and A. G. Piersol 1971 *Random Data: Analysis and Measurement Procedures*. New York: Wiley-Interscience.
25. R. Singh and W. Soedel 1978 *Journal of Sound and Vibration* **56**, 105–125. An efficient method of measuring impedances of fluid machinery manifolds.

APPENDIX: NOMENCLATURE

A, B, C, D	four-pole matrix coefficients
c	speed of sound
j	imaginary unit, $=\sqrt{-1}$
k	number of cylinders
l	length
$\dot{m}$	mass flow rate through the discharge valve
n	harmonic number
N	total number of harmonics
p	pressure
S	cross-sectional area
t	time
$\dot{X}$	volume velocity
Z	acoustical impedance
γ	propagation constant
Δ	four-pole matrix of a circular finite tube
$\delta\theta$	crank angle resolution
θ	crank angle
ρ	fluid mean density
ϕ	crank phase between cylinders
ψ	phase of a complex quantity
ω	compressor running speed, radian frequency
β	damping factor

Subscripts

a	anechoic line
i	cylinder index
r	general index; denotes both cylinder number $(r = 1, 2, \ldots, k)$ and input to a dynamic system
q	general index; denotes both cylinder number $(r = 1, 2, \ldots, k)$ and output of a dynamic system
v	valve chamber
1–14	elements of the example case presented in Figure 3

Superscript

	denotes complex quantity